JACS
JOURNAL OF THE AMERICAN CHEMICAL SOCIETY
Article
pubs.acs.org/JACS

Anion–π Catalysis

Yingjie Zhao, César Beuchat, Yuya Domoto, Jadwiga Gajewy, Adam Wilson, Jiri Mareda, Naomi Sakai, and Stefan Matile*

Department of Organic Chemistry, University of Geneva, Geneva, Switzerland

Supporting Information

ABSTRACT: The introduction of new noncovalent interactions to build functional systems is of fundamental importance. We here report experimental and theoretical evidence that anion–π interactions can contribute to catalysis. The Kemp elimination is used as a classical tool to discover conceptually innovative catalysts for reactions with anionic transition states. For anion–π catalysis, a carboxylate base and a solubilizer are covalently attached to the π-acidic surface of naphthalenediimides. On these π-acidic surfaces, transition-state stabilizations up to $\Delta\Delta G_{TS}$ = 31.8 ± 0.4 kJ mol^{-1} are found. This value corresponds to a transition-state recognition of K_{TS} = 2.7 ± 0.5 μM and a catalytic proficiency of 3.8 × 10^5 M^{-1}. Significantly increasing transition-state stabilization with increasing π-acidity of the catalyst, observed for two separate series, demonstrates the existence of "anion–π catalysis." In sharp contrast, increasing π-acidity of the best naphthalenediimide catalysts does not influence the more than 12 000-times weaker substrate recognition (K_M = 34.5 ± 1.6 μM). Together with the disappearance of Michaelis–Menten kinetics on the expanded π-surfaces of perylenediimides, this finding supports that contributions from π–π interactions are not very important for anion–π catalysis. The linker between the π-acidic surface and the carboxylate base strongly influences activity. Insufficient length and flexibility cause incompatibility with saturation kinetics. Moreover, preorganizing linkers do not improve catalysis much, suggesting that the ideal positioning of the carboxylate base on the π-acidic surface is achieved by intramolecular anion–π interactions rather than by an optimized structure of the linker. Computational simulations are in excellent agreement with experimental results. They confirm, *inter alia*, that the stabilization of the anionic transition states (but not the neutral ground states) increases with the π-acidity of the catalysts, i.e., the existence of anion–π catalysis. Preliminary results on the general significance of anion–π catalysis beyond the Kemp elimination are briefly discussed.

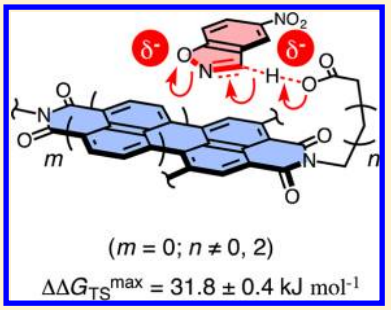

INTRODUCTION

The underappreciation of anion–π interactions is understandable.[1−9] Classical aromatic rings are characterized by clouds of π electrons that accumulate above and below the plane of the atoms in the ring. The resulting negative quadrupole moments Q_{zz} < 0 are characteristic for π-basic aromatics and compatible with the interaction with cations rather than anions (Figure 1a). Benzene, for example, has a quadrupole moment of −9 Buckinghams (Q_{zz} = −9 B, Figure 1c). To invert the intrinsic negative quadrupole moment of aromatic rings, strongly withdrawing substituents are needed. The resulting π-acidic aromatics with Q_{zz} > 0 have an electron-poor surface that should, in principle, attract anions (Figure 1b). The arguably most popular example for π-acidic aromatics is hexafluorobenzene with Q_{zz} = +10 B (Figure 1d). Early on, we realized that naphthalenediimides (NDIs)[4] would be ideal to study anion–π interactions because their quadrupole moments are very large.[5] Already the native NDI has with Q_{zz} = +19 B a quadrupole moment that is in the range of TNT (Figure 1e).[5] The introduction of two cyano groups in the NDI core gives with Q_{zz} = +39 B the strongest π-acid known today (Figure 1f).[6] Four cyano groups should provide access to Q_{zz} = +55 B, but the synthesis of these super-π-acids has so far not been successful, their aromatic core is probably too electron deficient to exist (Figure 1g).[6,7] The magnitude of these quadrupole moments can vary significantly with the method of calculation used. However, the relative trends are always the same.

The quadrupole moments of NDIs with sulfides and sulfoxides in the core have not been calculated so far because of open questions concerning their axial symmetry.[8,9] However, the higher energy of their LUMO at −3.93 eV compared to −4.31 eV of unsubstituted NDIs implies that electron-donating sulfide substituents reduce the π-acidity of these NDIs (Figure 1i).[8] Q_{zz} = +8 B with alkoxy and Q_{zz} = +2 B with alkylamino substituents in the core demonstrate that NDIs with sulfides in the core remain π-acidic.[10] NDIs with sulfides in the core are interesting because their oxidation to sulfoxides and sulfones converts the π-donors into π-acceptors.[8] The drop of their LUMO energy level from −3.93 eV to −4.46 eV in response to sulfide oxidation suggests that the π-acidity with two sulfoxides in the core should be localized between that of native and dicyano NDIs (Figure 1j).[8] Because the effect of the imide acceptors is diluted over a larger surface, the LUMO energy level of native perylenediimides (PDIs)[11] is with −4.20 eV above that of native NDIs at −4.31 eV (Figure 1h).[4] This suggests that compared to NDIs, anion–π interactions with

Received: December 6, 2013
Published: January 23, 2014

   dx.doi.org/10.1021/ja412290r | J. Am. Chem. Soc. 2014, 136, 2101−2111

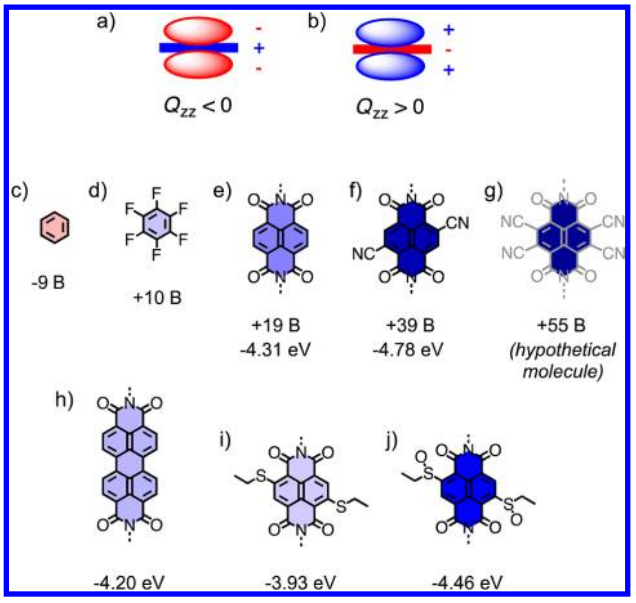

Figure 1. Schematic side view of (a) π-basic and (b) π-acidic aromatic rings (solid lines) with their electron-poor (blue) and -rich (red) π-clouds, and (c–j) representative examples with their axial quadrupole moments Q_{zz} in Buckinghams B or their LUMO energy against −5.1 eV for Fc/Fc^+.

PDIs should be weaker, whereas π–π interactions are much stronger.

The first explicit theoretical considerations of interactions between anions and π-acidic aromatics appeared about one decade ago.[1] Considering different ways anions can interact with π-acidic aromatics, extensive discussions concerning the exact nature of anion–π interactions continue today.[2] Early on, these theoretical studies could be supported by observations in crystals, but proximity in the solid can originate from effects other than anion–π interactions. It was quite difficult to observe and characterize anion–π interactions in solution, and they still remain somewhat elusive.[3] Even harder to catch them at work, direct experimental evidence for their functional relevance was secured only 4 years ago.[6] This breakthrough was possible using synthetic transport systems as unique analytical tools to elaborate on more elusive interactions such as anion–π interactions or halogen bonds.[6,8,12] Experimental evidence for anion–π interactions at work in transport implied that they should also be useful for catalysis. Stabilization of anions in the ground state suggests that the same process can stabilize anionic transition states. The perspective to use anion–π interactions in catalysis was interesting. The complementary, much more popular cation–π interactions[13] have been implicated in the stabilization of carbocation intermediates in biosynthetic routes, including terpene cyclizations.[14] Cation–π interactions also have been used quite extensively in organocatalysis.[15] In sharp contrast, anion–π interactions are essentially[16] unknown in catalysis.

The introduction of new interactions for the design of new catalysts, or new functional systems in general, is of fundamental importance. Simply speaking, hydrogen bonds, hydrophobic interactions, π–π interactions, ion pairing, and cation–π interactions can be considered as basic set available to engineer interactions between and within molecules. In organocatalysis, emphasis is on hydrogen bonds, sometimes used in concert with hydrophobic contacts and π–π and cation–π interactions.[15] Ion pairing receives much current attention.[17] Moreover, reports on catalysis with halogen bonds[12,18] and new aspects of dynamic covalent bonds[19] continue to emerge. Building on a recent communication of preliminary results,[20] we here report experimental and theoretical evidence that anion–π interactions can contribute to catalysis.

RESULTS AND DISCUSSION

Initial Results.[20] The Kemp elimination was selected for initial studies on possible contributions of anion–π interactions to catalysis. This choice was made because the Kemp elimination has emerged as an ideal analytical tool to elaborate on conceptually innovative catalysts.[21] Examples include theoretically designed enzymes, catalytic antibodies, promiscuous proteins, synthetic polymers, macrocyclic model systems, vesicles, micelles, and nonspecific medium effects. There is consensus in the field that the Kemp elimination is completely useless with regard to practical applications in organocatalysis. However, this concern is obviously irrelevant for the topic of this study.

The key to "anion–π catalysis" was to place a carboxylate base on the π-acidic surface of catalyst **C** (Figure 2). With this architecture, the onset of anion–π interactions could coincide with the injection of the negative charge into the substrate. In transition state **TS**, the negative charge could flow over the π-acidic surface from the carboxylate base over the carbanion of the conjugate base to the phenolate oxygen. Moreover, proton

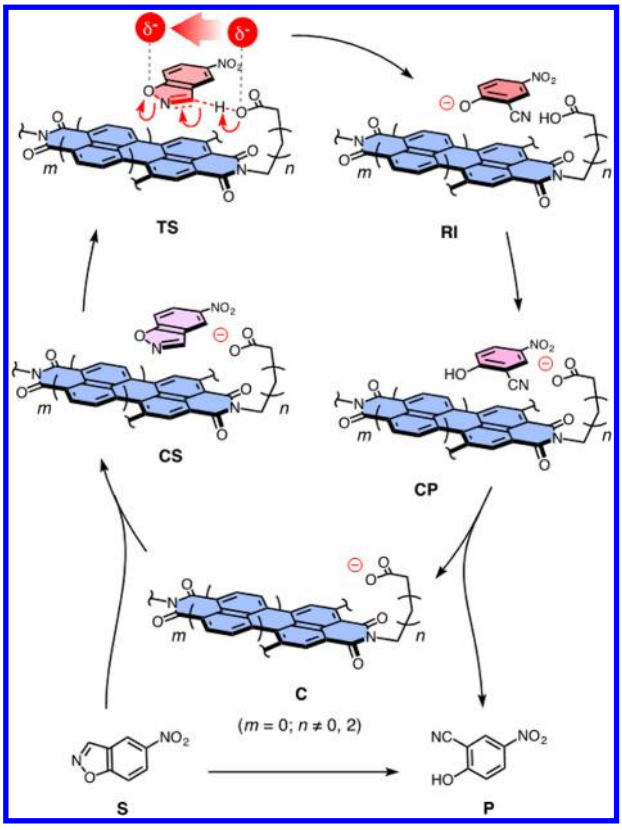

Figure 2. Design of anion–π catalysts **C** emphasizes a carboxylate base on a π-acidic surface to couple charge injection into the substrate **S** with the onset of transition-state (**TS**) stabilization by anion–π interactions and to prevent product inhibition (blue = electron deficient, red = electron rich, **CS** = catalyst–substrate complex, **RI** = reactive intermediate, **CP** = catalyst–product complex).

dx.doi.org/10.1021/ja412290r | J. Am. Chem. Soc. 2014, 136, 2101–2111

transfer from the carboxylic acid to the phenolate in **RI** would prevent product inhibition and regenerate the catalyst **C**. Catalysis in its broadest sense is understood as transition-state stabilization.[22] Catalyst **C**, offers anion−π interactions to stabilize the anionic transition state **TS**. Acceleration of the Kemp elimination by catalyst **C** would, therefore, prove the existence of anion−π catalysis.

To elaborate on these expectations, catalyst **1** was synthesized first (Figure 3). A carboxylate base and a

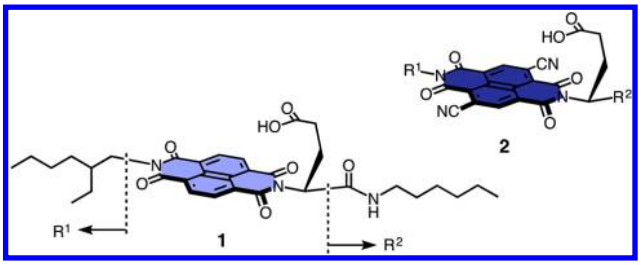

Figure 3. Structure of catalysts **1** and **2**.

solubilizing alkyl tail are attached to a π-acidic surface of NDI **1**. Contrary to all controls, catalyst **1** showed saturation behavior. Michaelis−Menten analysis[22] gave a ground-state stabilization of $\Delta\Delta G_{GS}$ = 6.2 ± 0.2 kJ mol^{-1} and a transition-state stabilization of $\Delta\Delta G_{TS}$ = 28.3 ± 0.4 kJ mol^{-1}. This corresponds to a transition-state recognition of K_{TS} = 10.9 ± 1.6 μM in MeOH/$CHCl_3$ 1:1.

If anion−π interactions indeed stabilize the transition state of the Kemp elimination, increasing π-acidity should result in increasing activity. Catalyst **2** is identical with catalyst **1** except for the two cyano substituents in the NDI core. This increase in π-acidity without global structural change gave a transition-state stabilization of $\Delta\Delta G_{TS}$ = 30.3 ± 0.4 kJ mol^{-1}. An increase of $\Delta\Delta\Delta G_{TS}$ = 2.0 kJ mol^{-1} was exactly as expected for strengthened anion−π interactions in the transition state stabilized by catalyst **2**.

Theoretical Considerations. We have examined the most important aspects of the anion−π catalyzed Kemp elimination by theoretical DFT calculations using the well-tested and dispersion-corrected B97-D functional.[23] While B97-D functional provides good geometries, binding energies of complexes are often overestimated. Therefore for energy calculations we used M06-2X meta-hybrid functional,[24] which provide good results for both thermodynamics as well as kinetics. For all calculations the solvation by chloroform was taken into account with IEFPCM model.[25] For modeling purposes, the structures of catalysts **1** and **2** were simplified by removing the solubilizing alkyl tails with R^1 = CH_3, R^2 = H (Figure 3). The Leonard linker connecting the carboxylate base to NDI of catalysts **1** and **2** breaks the symmetry of complexes between the catalyst and benzisoxazole. Therefore the two different orientations of benzisoxazole **S** can occur within the catalyst−substrate complex, leading to the isomers **CS1** and **CS1′** where the orientation of benzisoxazole **S** is inversed (Figure 4). Because of asymmetric character of the linker and substrate, one must also distinguish between two different dicyano-substitution patterns for the naphthyl core: the formally 3,7-dicyano- and 2,6-dicyano-substituted complexes **CS2** and **CS2′**, respectively (Figure 4).

Among all possible structures of the initial catalyst−substrate complexes, **CS1** and **CS2** proceed with the lowest-energy pathways toward the transition state of the Kemp elimination

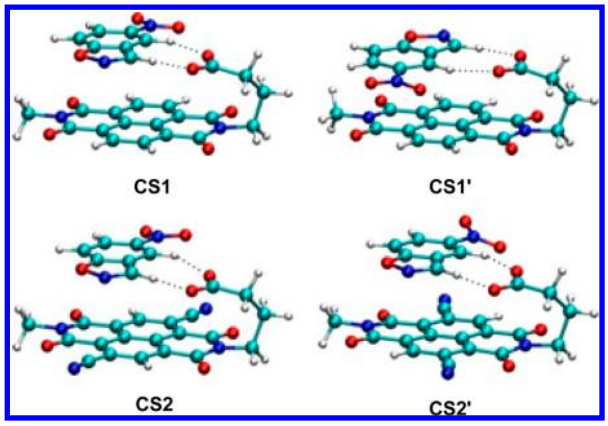

Figure 4. Optimized structures (IEFPCM/B97-D/6-311G**) of most significant low energy catalyst−substrate complexes.

(Figure 4). Already in the early stage of the reaction, i.e., in catalyst−substrate complex **CS1**, the carboxylate anion is positioned so that efficient intramolecular anion−π interactions with the most π-acidic part of NDI surface can take place. The coplanar arrangement between the carboxylate and NDI planes, apart by 3.035 Å, suggests a contribution also from π−π interactions. The carboxylate anion of the catalyst also plays a role in anchoring the benzisoxazole substrate above the NDI surface via two C−H···O interactions (1.887 and 2.218 Å, respectively), therefore favoring the π−π interactions between the two coplanar aromatic systems. This perfectly sets the stage for the proton transfer between the catalyst and the substrate, leading eventually to early transition state **TS1** with the activation barrier of 62.9 kJ mol^{-1} (Figure 5a). At this stage the electron transfer occurring over several atoms from carboxylate anion to phenolate oxygen is efficiently stabilized by the π-acidic surface of NDI. In accordance with the anion−π stabilization, the buildup of negative charge of phenolate oxygen, which effectively doubles to −0.3672, is accompanied

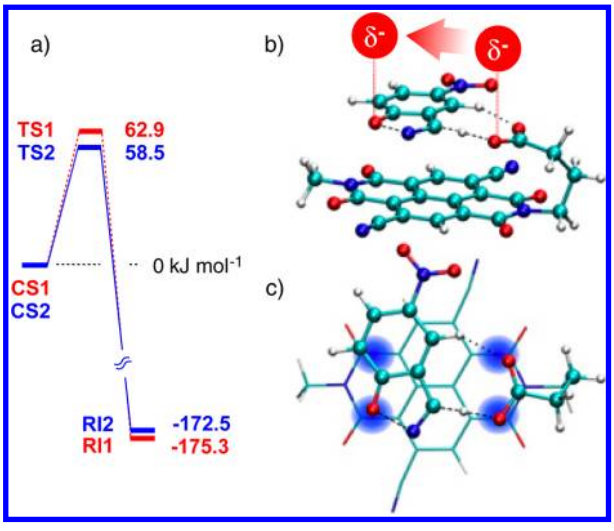

Figure 5. (a) Free energy diagram (IEFPCM/M06-2X/def2-TZVP//IEFPCM/B97-D/6-311G**) for the Kemp elimination with anion−π catalyst **1** (in red) and **2** (in blue). (b) Optimized structure of the transition state (**TS2**) for the reaction catalyzed by catalyst **2**, negative charge transfer is highlighted in red. (c) Axial view of **TS2** showing optimal overlap of centers where the electron transfer takes place with the preferential binding sites (in blue) of π-acidic NDI.

dx.doi.org/10.1021/ja412290r | J. Am. Chem. Soc. 2014, 136, 2101−2111

by decreasing distance of the oxygen atom from the NDI surface going from 3.276 to 3.202 Å.

The NDI catalyst is ideally suited for the charge injection into substrate since it can simultaneously accommodate the carboxylate and the phenolate oxygen, both overlapping with the distinct preferential binding sites (blue spots in Figure 5c). Such sites have been identified for NDI−halide anionic complexes,[6] knowing that in general for π-acidic aromatic systems the totality of their surface can interact favorably with anions.[26] The reaction progresses toward the anionic intermediate **RI1**, while the negative charge is fully transferred to the benzisoxazole substrate. The benzisoxazole oxygen accumulates most of the charge (−0.6456), while its distance from the NDI surface further decreases to 2.995 Å. The conformation of this complex once again favors anion−π interactions by placing the anionic oxygen right above the preferential binding site of NDI, therefore stabilizing the complex.

The Kemp elimination in the presence of the 3,7-dicyano-substituted catalyst **2** follows a similar pathway as with catalyst **1**. However, the increased π-acidity enhances the **TS2** transition-state stabilization by 4.4 kJ mol^{-1} when compared to **TS1** (Figure 5a). While the energy differences are quite small, this stabilization is only about 2.4 kJ mol^{-1} stronger than what was experimentally measured for catalyst **2**[20] and the sulfoxide-substituted catalyst **4** (see below). Convincing stabilization enhancement of **TS2** by more π-acidic NDI surface of **2** confirms that anion−π interactions contribute significantly to this reaction. As was the case for **TS2**, the reaction is again favored by perfect alignment of the negative charge transfer between the carboxylate base and substrate and preferential binding sites of the π-acidic surface of NDI in the **TS2** (Figure 5c). The evolution of certain geometric parameters during the reaction mechanism involving catalyst **2** also reflects enhanced anion−π implication; namely the more pronounced decrease of the distance between benzisoxazole oxygen and NDI plane from 3.154 Å in **CS2** to 3.046 Å in **TS2** to contract finally to 2.804 Å in **RI2** and is correlated with the negative charge buildup of −0.455 on the phenolate oxygen. When compared to mechanism involving less π-acidic catalyst **1**, yet another structural difference is the slight reduction of interplanar distances between the two π-systems; for transition states by 0.032 Å and for reactive intermediates by 0.026 Å.

It is also noteworthy to mention that the potential energy surfaces showed slightly higher activation barriers for Kemp elimination in case of structures where benzisoxazole was inverted in substrate−catalyst complexes (see the conformer **CS2′** in Figure 4). Nevertheless, the transition-state stabilization of 1.7 kJ mol^{-1}, upon dicyano substitution of the naphthyl core, was also detected in such alternate conformation. Interestingly enough the majority of conformers displayed better overlap of benzisoxazole phenyl ring with NDI π-system but only at the expense of slightly disfavoring the interactions of benzisoxazole oxygen with the preferential binding site of NDI. This could explain the slightly higher energy pathways for these conformers since improved π−π interactions do not fully compensate for weaker anion−π interactions. For the 2,6-dicyano-substituted substrate−catalyst complex **CS2′** (Figure 4), the activation barrier is also higher than for the 3,7-disubstituted complex **CS2** discussed above.

In order to appreciate binding energies at the transition state of the Kemp elimination catalyzed by **1** or **2**, we designed a model system, where the carboxylate base and the linker were removed keeping only the substrate and the *N*,*N*-dimethyl NDI, as a simplified surrogate for the catalyst. The overall structure of this model complex was constrained in the geometry of the corresponding transition state (**TS1** or **TS2**), while the interaction energy was computed with the BSSE correction. For the neutral complex between the benzisoxazole and *N*,*N*-dimethyl-3,7-dicyano NDI, the computed binding energy of −32.4 kJ mol^{-1} is mostly reflecting the π−π interactions (Figure 6a, entry 2). When in the neutral complex

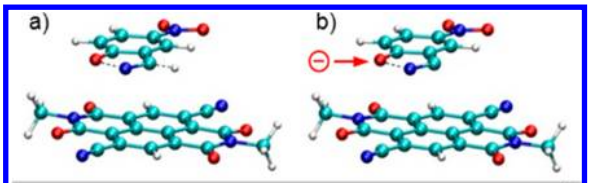

Entry	Complex	*Charge*	E_{int} (kJ mol^{-1})
1	NDI benzisoxazole	0	-34.3
2	3,7-dicyano-NDI benizoxazole	0	-32.4
3	NDI benzisoxazole	-1	-51.0
4	3,7-dicyano-NDI benizoxazole	-1	-69.2

Figure 6. Model for transition-state complexes of (a) neutral and (b) negatively charged complexes of benzisoxazole with *N*,*N*-dimethyl NDI. For both unsubstituted and dicyano-substituted substrates the BSSE corrected binding energies are computed with the IEFPCM/M06-2X/Def2-TZVP method.

cyano substituents on the NDI are removed, the binding energy increases by 1.9 kJ mol^{-1} (Figure 6a, entry 1). Remarkably, upon dicyano NDI substitution of anionic complexes a substantial increase of binding energy is noted. It increases from −51.0 to −69.2 kJ mol^{-1}, highlighting the anion−π interaction enhancement with increased π-acidity of NDI surface (Figure 6b, entries 3 and 4). This simplified model confirms in a more prominent way the transition-state stabilization occurring via anion−π interactions in a subtler manner during the Kemp elimination catalyzed by **1** and **2**.

Dependence of Anion−π Catalysis on π-Acidity. The most convenient method to increase π-acidity without global structural changes uses sulfide oxidation chemistry.[8,9] With *m*-chloroperbenzoic acid (MCPBA), sulfide donors can be converted in situ into sulfoxide and sulfone acceptors. This strategy has been used to build voltage-gated ion channels[27] and to produce NDIs with maximal π-acidity under mild conditions.[8] To apply this strategy to anion−π catalysis, the weakly π-acidic NDI **3** with two sulfides in the core was envisioned (Figure 7). Oxidation under mild conditions will afford the strong π-acid **4** with two sulfoxides in the core, further oxidation would give two sulfones. Compared to the introduction of cyano groups in catalyst **2**, this approach was attractive because the increase in π-acidity occurs with minimal global structural change.

The synthesis of catalyst **3** from naphthalenedianhydride (NDA) **5** was mostly straightforward (Scheme 1). Building on experience with related systems, NDA **5** was brominated first.[4,28] The reaction mixture including the desired 2,6-dibromo NDA **6** was used without further purification. Reaction with the two amines **7** and **8** gave mixed NDI **9** together with the symmetrical side products. The bromo substituents in the NDI core of **9** were finally replaced by sulfides. This nucleophilic aromatic substitution with thioethanol nicely illustrates the intrinsic π-acidity of the NDI core.

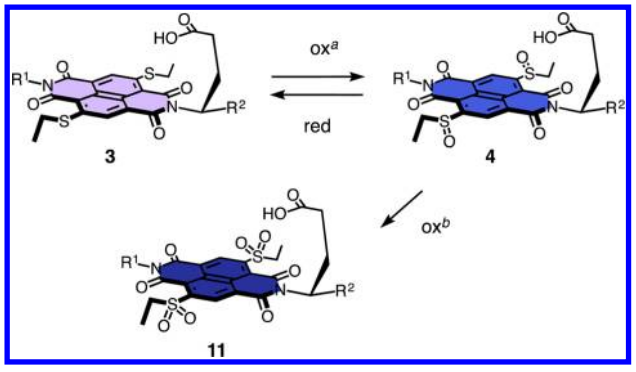

Figure 7. Structure of the catalysts **3** and **4**. R^1 and R^2 as in Figure 3. (a) MCPBA, CH_2Cl_2, 0 °C; and (b) MCPBA, CH_2Cl_2, room temperature.

Scheme 1. Synthesis of catalyst 3[a]

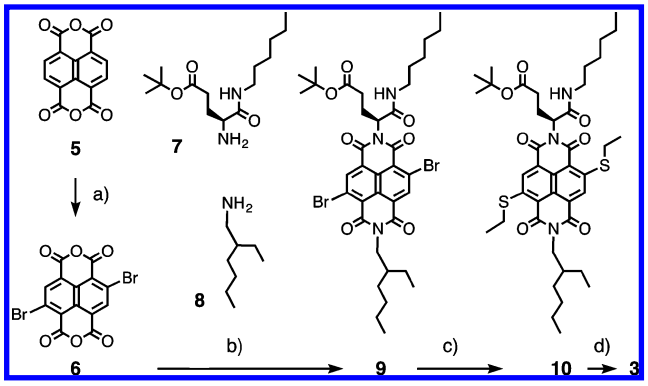

[a](a) Dibromoisocyanuric acid, H_2SO_4, rt, 12 h, 76%;[4,28] (b) AcOH, 80 °C; (c) EtSH, 18-crown-6, K_2CO_3, $CHCl_3$, 75 °C; (d) TFA, CH_2Cl_2.

Deprotection of the acid in NDI **10** afforded catalyst **3**, which could be oxidized to catalyst **4** with MCPBA at 0 °C. MCPBA oxidation at room temperature lead directly to the corresponding sulfone **11**. Unfortunately, the NDI **11** with maximal π-acidity could not be used for catalysis because of the onset of competing, unidentified side reactions.

The influence of the π-acidic NDIs **3** and **4** on the kinetics of the Kemp elimination was followed by ^{1}H NMR spectroscopy (Figure S1). This choice was important because one of the advantages of the Kemp elimination is that it can be followed by absorption spectroscopy. However, ^{1}H NMR spectroscopy was preferable because the higher concentrations needed under routine conditions revealed saturation kinetics also for systems with weak ground-state stabilization, i.e., Michaelis constants K_M in the millimolar range. The conditions developed to characterize catalysts **1** and **2** were used without change to ensure comparability, i.e., solutions of catalysts (8.3 mM), TBAOH (5.0 mM), and substrate **S** (0–180 mM) in CD_3OD/$CDCl_3$ 1:1, stirred at room temperature.

The initial velocities of product formation v_{ini} were determined as a function of the substrate concentration [**S**]. The catalytic activity clearly increased with increasing π-acidity from catalyst **3** (Figure 8, ○) to catalyst **4** (Figure 8, ●). Curve fit to eq 1:

$$v_{ini}/[\mathbf{C}] = k_{cat}[\mathbf{S}]/(K_M + [\mathbf{S}]) \quad (1)$$

gave the rate constants k_{cat} and the Michaelis constants K_M. The latter correspond to the dissociation constants in the ground states, i.e., the catalyst–substrate complexes **CS** (Figure 2). The

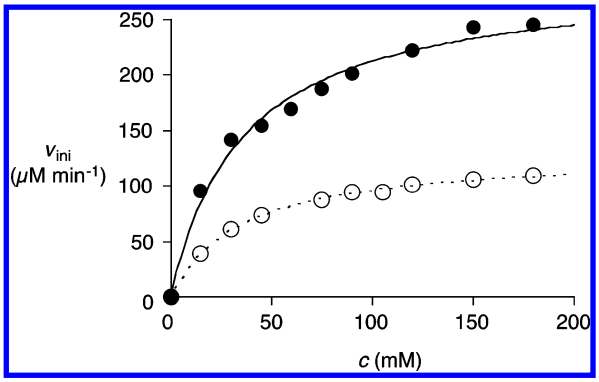

Figure 8. Initial velocity of product formation as a function of the concentration of substrate **S** in the presence of 8.3 mM **3** (○) and **4** (●); 5.0 mM TBAOH, CD_3OD/$CDCl_3$ 1:1, room temperature; with Michaelis–Menten curve fit.

formal dissociation constants of the transition states **TS**, i.e., K_{TS}, were approximated with eq 2:

$$K_{TS} = k_{non}K_M/k_{cat} \quad (2)$$

where k_{non} is the rate constant of the uncatalyzed Kemp elimination under identical conditions (i.e., $k_{non} = (7.1 \pm 0.1) \times 10^{-8}$ s^{-1}).[20] From the dissociation constants of the transition states K_{TS}, the transition-state stabilizations $\Delta\Delta G_{TS}$ were readily approximated with eq 3:

$$\Delta\Delta G_{TS} = -RT\ln K_{TS} \quad (3)$$

The ground-state stabilizations $\Delta\Delta G_{GS}$ were approximated analogously from K_M. The results of the Michaelis–Menten analysis for catalysts **3** and **4** are summarized in Table 1 and Figure 9.

Compared to the original NDI **1**, the introduction of sulfide π-donors in the core of NDI **3** increased the ground-state stabilization by +2.1 kJ mol^{-1} (Table 1, entries 1 and 3). This anticatalytic effect suggested that hydrophobic contacts with the ethyl groups at the periphery are sufficient to overcompensate weakened π–π interactions. This was the first indication that changes in π-acidity influence π–π interactions much less than anion–π interactions. The validity of this important conclusion was nicely confirmed by the observation that, compared to NDI **1**, the stabilization of the transition state by NDI **3** was with +1.6 kJ mol^{-1} slightly weaker than that of the ground state (Table 1, entries 1 and 3).

The increase in π-acidity upon oxidation of catalyst **3** to **4** caused an increase in transition-state stabilization by +1.9 kJ mol^{-1} (Table 1, entries 3 and 4, Figure 9). In other words, the recognition of the transition state increased from $K_{TS} = 5.7 \pm 0.4$ μM for **3** to $K_{TS} = 2.7 \pm 0.5$ μM for **4**. This increase was nearly the same as the one observed previously with catalysts **1** and **2** (+2.0 kJ mol^{-1}, Table 1, entries 1 and 2). This finding provided powerful corroborative evidence for the existence of anion–π catalysis.

Most importantly, the increase in π-acidity from catalyst **3** to **4** did not cause an increase in ground-state stabilization (Table 1, entries 3 and 4, Figure 9). This finding was in sharp contrast to the previously reported catalysts **1** and **2**. In that system, increasing transition-state stabilization by +2.0 kJ mol^{-1} coincided with increasing ground-state stabilization by +0.9 kJ mol^{-1} (Table 1, entries 1 and 2). This ground-state stabilization could originate from increasing π–π interactions with increasing π-acidity or peripheral contacts with the added

dx.doi.org/10.1021/ja412290r | J. Am. Chem. Soc. 2014, 136, 2101–2111

Table 1. Characteristics of Anion–π Catalysts[a]

entry	catalyst	K_{TS} (μM)[b]	K_M (mM)[c]	$(k_{cat}/K_M)/k_{non}$ (M^{-1})[d]	$\Delta\Delta G_{TS}$ (kJ mol^{-1})[e]	$\Delta\Delta G_{GS}$ (kJ mol^{-1})[f]
1[g]	**1**	10.9 ± 1.6	82.5 ± 7.8	92000	28.3 ± 0.4	6.2 ± 0.2
2[g]	**2**	5.0 ± 0.8	56.5 ± 6.2	200000	30.3 ± 0.4	7.1 ± 0.3
3	**3**	5.7 ± 0.4	34.5 ± 1.6	176000	29.9 ± 0.2	8.3 ± 0.1
4	**4**	2.7 ± 0.5	35.9 ± 4.5	384000	31.8 ± 0.4	8.3 ± 0.3
5	**12**	5.4 ± 1.4	31.0 ± 5.4	197000	30.1 ± 0.6	8.6 ± 0.4
6[h]	**13**	na[h]	na[h]	na[h]	na[h]	na[h]
7	**14**	10.6 ± 2.2	63.4 ± 8.5	99000	28.5 ± 0.4	6.9 ± 0.3
8	**15**	19.3 ± 3.5	115.9 ± 12.7	53000	26.9 ± 0.5	5.4 ± 0.3
9	**16**	5.1 ± 1.2	37.6 ± 6.3	205000	30.2 ± 0.6	8.2 ± 0.4
10	**17**	5.6 ± 2.1	41.5 ± 11.3	208000	30.2 ± 1.0	8.0 ± 0.5
11	**18**	3.9 ± 1.0	26.6 ± 5.0	270000	30.9 ± 0.6	9.0 ± 0.5
12	**20**	na[h]	na[h]	na[h]	na[h]	na[h]
13	**21**	20.8 ± 4.0	142.8 ± 16.2	50000	26.8 ± 0.5	4.8 ± 0.3
14	**22**	na[h]	na[h]	na[h]	na[h]	na[h]

[a]From Michealis–Menten analysis, compare Figures 8, 9, 11, and 13 and eqs 1–3. [b]Dissociation constant of the transition state **TS** (Figure 2) from eq 2. [c]Michaelis constant, comparable to the dissociation constant of the catalyst–substrate complex **CS** (Figure 2) from eq 1. [d]Catalytic proficiency, from eq 1, $k_{non} = 7.1 \times 10^{-8}$ s^{-1}.[20] [e]Transition-state stabilization from eq 3. [f]Ground-state stabilization, from $\Delta\Delta G_{GS} = -RT \ln K_M$. [g]Data from ref 20. [h]na = not applicable; these catalysts did not show saturation kinetics.

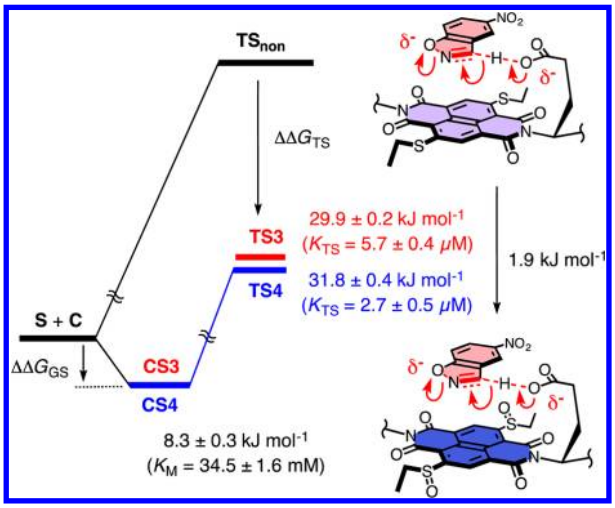

Figure 9. Energy diagram for the Kemp elimination catalyzed by anion–π catalysts **3** and **4** (compare Figure 8 and Table 1).

cyano groups. The insensitivity of the ground-state stabilization to increasing π-acidity of catalysts **3** and **4** with nearly identical global structure supported that the latter is the case. This finding was important because it confirmed that the impact of increasing π-acidity on anion–π interactions exceeds that on π–π interactions by far. The key conclusion that increasing transition-state stabilization with increasing π-acidity demonstrates the existence of anion–π catalysis therefore holds. Results from computational studies are in agreement with this conclusion (see above).

The new anion–π catalyst **4** is the most performant anion–π catalyst prepared so far. The $\Delta\Delta G_{TS}$ = 31.8 ± 0.4 kJ mol^{-1} corresponds to a recognition of the anionic transition state with K_{TS} = 2.7 ± 0.5 μM. This quite remarkable transition-state recognition by anion–π interactions exceeds the recognition of the neutral substrate by a factor of more than 12000 (K_M = 35.9 ± 4.5 mM). The transition-state stabilization $\Delta\Delta G_{TS}$ = 31.8 ± kJ mol^{-1} by the so far best anion–π catalyst **4** corresponds to a catalytic proficiency $(k_{cat}/K_M)/k_{non} = 3.8 \times 10^5$ M^{-1} (Table 1). With increasing π-acidity, the catalytic proficiency more than doubled from $(k_{cat}/K_M)/k_{non} = 1.8 \times 10^5$ M^{-1} for **3** to $(k_{cat}/K_M)/k_{non} = 3.8 \times 10^5$ M^{-1} for **4**.

In NDI **4**, the sulfoxides exist as mixtures of stereoisomers. The possibility to separate these stereoisomers has been demonstrated previously, and the anion-transport activity of individual stereoisomers differed significantly.[9] These results imply that enantiopure anion–π catalysts **4** would be even better catalysts. Moreover, they identify catalysts **4** with achiral π-surfaces as attractive starting point for developments toward asymmetric anion–π catalysis.

Dependence of Anion–π Catalysis on Solubilizers. In the original anion–π catalyst **1**, one imide of the NDI carries the carboxylate base, whereas the other is equipped with a branched alkyl substituent in racemic form (Figure 3). This partial "swallowtail" is essential to solubilize the catalyst. To evaluate possible contributions to anion–π catalysis, alternative solubilizers had to be explored. In NDI **12**, the original solubilizer was replaced by a π-basic phenyl group with two solubilizing alkoxy substituents in *meta* and *para* position (Figure 10).

Compared to original anion–π catalyst **1**, the presence of the aromatic solubilizer in NDI **12** increased the ground-state stabilization by +2.4 kJ mol^{-1} (Table 1, entries 1 and 5). This substrate recognition conceivably originated from hydrophobic contacts between the benzisoxazole and the aromatic solubilizer. A significant C–H···O bond to the benzisoxazole oxygen is less likely because the increase in transition-state stabilization $\Delta\Delta G_{TS}$ by anion–π catalysts **1** and **12** was the about same as for the ground state (Table 1, entries 1 and 5). The stabilizing contributions of the new aromatic solubilizer in anion–π catalyst **12** were more prevalent in the ground state than the transition state and thus anticatalytic.

Dependence of Anion–π Catalysis on the Leonard Linker. In anion–π catalysts **1**–**4**, the carboxylate base is placed on the π-acidic surface with a Leonard linker (Figure 3).[29] This fully flexible propylene or trimethylene bridge has been identified early on as privileged structure to position motifs of interest on aromatic surfaces. The perfect topological matching offered by the Leonard linker has been used successfully to explore intramolecular π–π interactions,[29,30] cation–π interactions,[31,32] and arene-templated ion pair-

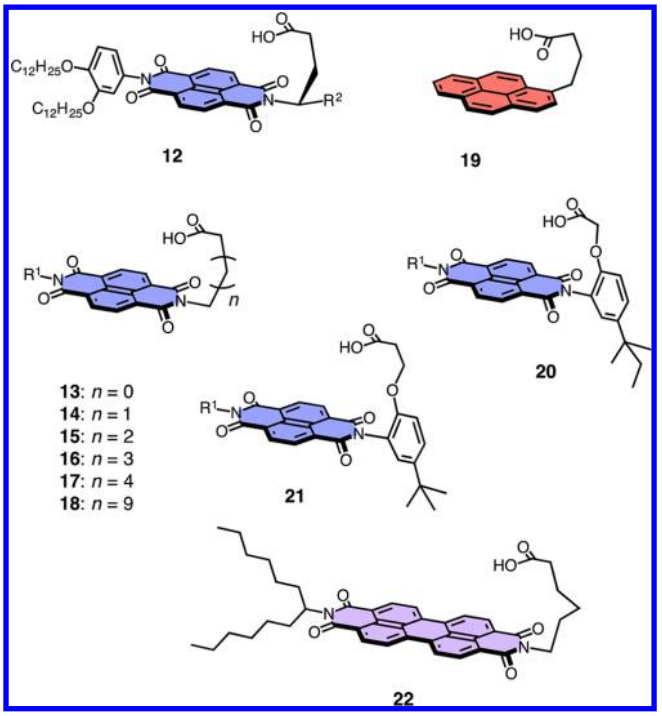

Figure 10. Structure of the catalysts **12**–**18** and **20**–**22** and of the cation–π control **19**. R^1 and R^2 are as in Figure 3.

ing,[32,17e] and the lessons learned have been applied to sensing[31] and cellular uptake.[32,17e] The robustness of the unusual U-motif of the Leonard linker has been confirmed in computational models, crystal structures, and in many variations.[29,30]

In the original anion–π catalyst **1**, L-glutamic acid is used to build a Leonard linker that places the carboxylate base on the π-acidic NDI surface (Figure 3). The second acid of L-glutamic acid is transformed into an amide that continues with a long, linear alkyl chain. The possible influence of the nature of this linker on solubility and activity of anion–π catalysts required clarification. Anion–π catalysts **13**–**18** contain simple alkyl linkers of increasing length (Figure 10).

Corresponding to the original NDI glutamic acid **1**, the NDI butyric acid **14** with a pure Leonard linker[29] gave nearly identical ground- and transition-state stabilizations (Figure 11, ●, Table 1, entries 1 and 7). This result demonstrated that the hexylamide branching in anion–π catalyst **1** is irrelevant for

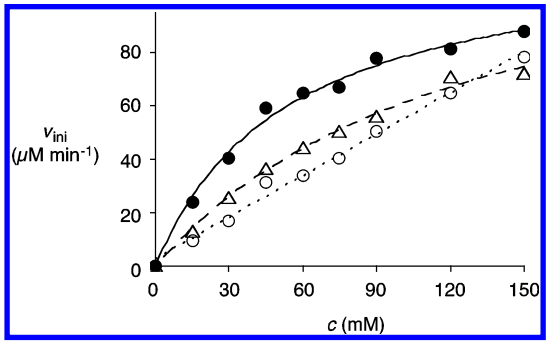

Figure 11. Initial velocity of product formation as a function of the concentration of substrate **S** in the presence of 8.3 mM catalyst **13** (○), **14** (●), and **15** (△), 5.0 mM TBAOH, $CD_3OD/CDCl_3$ 1:1, room temperature; with linear (○) and Michaelis–Menten curve fit (●, △, compare Table 1).

activity. It also confirmed that the catalytic inactivity of pyrenebutyrate **19** originates from anion–π repulsion with the π-basic pyrene and not from lacking substituents on the Leonard linker.[20]

Catalysis of the Kemp elimination by the NDI propionic acid **13** did not exhibit saturation kinetics (Figure 11, ○, Table 1, entry 6). This finding suggested that the propionate linker is too short to position the carboxylate on the π-acidic surface. The homologous NDI valeric acid **15** followed Michaelis–Menten kinetics (Figure 11, △). However, compared to the ideal NDI butyric acid **14**, ground-state stabilization $\Delta\Delta G_{GS}$ by the NDI valeric acid **15** dropped by −1.5 kJ mol^{-1} and transition-state stabilization $\Delta\Delta G_{TS}$ by −1.6 kJ mol^{-1} (Table 1, entries 7 and 8). This finding suggested that the valerate linker is too long to position the carboxylate correctly on the π-acidic surface.

These interpretations were well supported by molecular models (Figure 12). With the Leonard linker in butyrate **14**, the

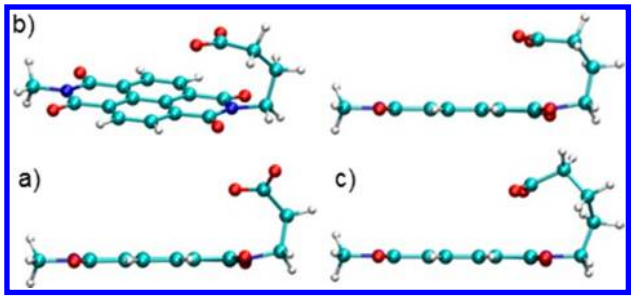

Figure 12. Optimized geometries (IEFPCM/B97D/6-311G**) of the deprotonated anion–π catalysts (a) **13**, (b) **14**, and (c) **15**; side views.

carboxylate anion resides comfortably on top of the most π-acidic pyridinedione heterocycle of the NDI (Figure 12b). Their separation by 2.88 Å is as expected for strong intramolecular anion–π interactions. The orientation of the carboxylate parallel to the NDI surface is consistent with the occurrence of π–π enhanced anion–π interactions. Similar observations have been made previously to explain the nitrate selectivity of anion transport with anion–π interactions.[3,6,12] A carboxylate lying parallel 2.88 Å above the π-acidic surface is ideal to contribute to the recognition of the benzisoxazole substrate. Dominated by π–π interactions, the proximal carboxylate has one oxygen lone pair in place for an important O···H–C bond to the benzene carbocycle and a second oxygen lone pair perfectly positioned to accept the proton from the isoxazole heterocycle and initiate the reaction (Figures 2 and 4).

Molecular models of mismatched NDI propionate **13** confirm that this linker is too short for π–π enhanced anion–π interactions with the π-acidic surface. As a result, the carboxylate reorients perpendicular to the NDI plane to position one lone pair for interaction with the π-surface (Figure 12a). This position of the carboxylate is obviously less suited to support substrate recognition and initiate the reaction.

Molecular models of mismatched NDI valerate **15** confirm that this linker is too long. The carboxylate has to bend down to the anion–π surface to establish intramolecular anion–π interactions (Figure 12c). These interactions misorient and partially use the lone pairs involved in catalysis.

Comparison with the mismatched **13** and **15** suggested that the Leonard linker in anion–π catalyst **14** is important for function (Table 1, entries 6–8). However, further elongation of

the linker restored catalytic activity to the fullest. With the NDI caproic acid **16**, $\Delta\Delta G_{GS}$ and $\Delta\Delta G_{TS}$ recovered by +2.8 and +3.3 kJ mol^{-1}, respectively (Table 1, entries 8 and 9). Compared to Leonard catalyst **14**, $\Delta\Delta G_{GS}$ and $\Delta\Delta G_{TS}$ of NDI caproic acid **16** were also clearly higher, although the increases mostly concerned counterproductive substrate recognition (Table 1, entries 7 and 9). Further linker elongation gave practically identical results with NDI enanthic acid **17** (Table 1, entry 10). The NDI lauric acid **18** with 11 carbons in the linker gave even slightly better activity, although the anticatalytic contributions from ground-state stabilization increased as well (Table 1, entry 11). Linker elongation also gradually decreased the solubility of the catalysts in the reaction mixture. The overall poor sensitivity of the anion–π catalysts to linker elongation beyond the critical length of five carbons in NDI caproic acid **16** indicated that the correct positioning of the carboxylate base on the π-acidic surface is mainly controlled by intramolecular anion–π interactions, whereas structural changes of the linker can hurt more than help. Shorter tails that interfere with this perfect positioning of the carboxylate reduce activity significantly (propionate **13**, valerate **15**). However, the perfect length of the Leonard liker in butyrate **14** does not have a pre-organizing effect, longer flexible chains give similar results (caproate **16** and beyond).

This interpretation was fully supported by catalysts with rigidified linkers. In catalyst **20**, the linker length is with four atoms identical with that of NDI valeric acid **15** (Figure 10). Already at full flexibility, this mismatched linker could not properly fold into a conformation that would allow for convincing intramolecular π–π enhanced anion–π interactions between carboxylate and π-acidic surface (Figure 12c). As a result, ground- and transition-state stabilization by anion–π catalyst **15** decreased (Table 1, entry 8). Further rigidification of this mismatched linkers in catalyst **20** gave very weak catalytic activity without saturation behavior, although pre-organization by the *ortho* substitution of the phenyl ring as such would point into the right direction (Table 1, entry 12).

Addition of one carbon in homologue **21** improved the situation. The Kemp elimination proceeded with saturation behavior, although ground- and transition-state stabilization remained comparably weak (Table 1, entry 13). The rigidified catalyst **21** was the weakest of all catalysts prepared, even catalyst **15** with a flexible but mismatched linker showed slightly better transition-state stabilization (Table 1, entry 8). This result supported the interpretation that catalytic activity is mainly governed by the correct positioning of the carboxylate above the π-acidic surface through intramolecular anion–π interactions and that any strain added in the linker hinders this positioning and thus reduces activity.

Perylenediimides. The inclusion of perylenediimides (PDIs)[11] in this study was of interest to better dissect contributions from π–π and anion–π interactions to catalysis. With an expanded π-surface, π–π interactions with PDIs are naturally stronger than with NDIs. In clear contrast, PDIs are less π-acidic than NDIs because the withdrawing effect of the two imides is diluted over the expanded π-surface. This decrease in π-acidity is illustrated by the increase of the energy of the LUMO (Figure 1).

In catalyst **22**, the PDI was equipped with a caproic acid as in the operational NDI catalyst **16** and a swallowtail solubilizer on the other side (Figure 10). This most powerful solubilizer was needed because the simpler solubilizer that was sufficient for the NDI catalysts failed to solubilize the PDI catalyst. Different solubilities nicely illustrate that the π–π interactions in PDIs are much stronger than in NDIs.[11] Catalysis of the Kemp elimination with PDI catalyst **22** did not exhibit saturation kinetics (Figure 13, ●; Table 1, entry 14). This incompatibility

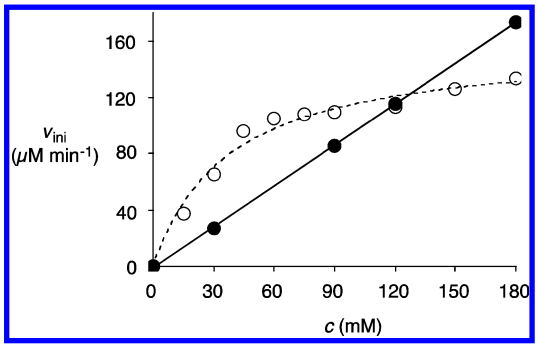

Figure 13. Initial velocity of product formation as a function of the concentration of substrate **S** in the presence of 8.3 mM catalyst **16** (○) and **22** (●), 5.0 mM TBAOH, $CD_3OD/CDCl_3$ 1:1 or 1:20, room temperature; with linear (●) and Michaelis–Menten curve fit (○, compare Table 1).

with Michaelis–Menten kinetics was in sharp contrast to the operational NDI catalyst **16** with the same caproate linker (Figure 13, ○; Table 1, entry 9). The dose response curve of the original NDI catalyst **1** is similar to that of **16**.[20] The relevant initial velocities at high dilution before the onset of saturation were clearly better for NDI catalyst **16** (or **1**) than for PDI catalyst **22** (Figure 13, left side). The poor performance of PDIs provided additional support that the contributions of π–π interactions to anion–π catalysis are nearly irrelevant. This finding was in agreement with insights from theory (Figures 4-6) as well as the independence of ground-state stabilization on increasing π-acidity (Figure 9).

■ CONCLUSIONS

In this study, compelling experimental evidence for the existence of catalysis with anion–π interactions is provided. The Kemp elimination is used as an established tool to elaborate on conceptual innovation in catalysis. Already very simple catalysts composed of a carboxylate base on top of a π-acidic naphthalenediimide (NDI) surface can accelerate this reaction. The best anion–π catalysts exhibit saturation behavior and are thus compatible with Michaelis–Menten analysis. This analysis reveals that the stabilization of the anionic transition state of the Kemp elimination increases with the π-acidity of the new catalysts. This finding, observed in two independent series, is very important because it demonstrates that anion–π interactions indeed contribute to catalysis. Computational studies support the key conclusion that transition-state recognition increases with increasing π-acidity of the catalyst.

This conclusion holds independent of the exact mode of anion recognition in the transition state. The intrinsic charge delocalization in any transition state implies that anion–π interactions in anion–π catalysis are necessarily beyond the strict definition of pure anion–π interactions. This situation stimulates continuing discussion on the nature of anion–π interactions and calls conceptual evolutions similar to the ones made in the perception of cation–π interactions, particularly when applied to catalysis.[13−15]

Contributions of π–π interactions to anion–π interactions were considered first to explain nitrate selectivity.[3,6,12] The

contributions from anion−π and π−π interactions to the acceleration of the Kemp elimination on π-acidic surfaces are not easily dissected. However, this study provides several surprising insights on this topic. Most importantly, anion−π catalysts were introduced that could change π-acidity without global structural changes (i.e., the oxidation of π-donating sulfides into π-accepting sulfoxides in the NDI core). With these catalysts, the stabilization of the neutral ground state is independent of the π-acidity of the catalyst, whereas that of the anionic transition state increases. Moreover, PDIs, characterized by stronger π−π and weaker anion−π interactions compared to NDIs, give catalysts that do not follow Michaelis−Menten kinetics. Computational studies confirm that π−π interactions are nearly insensitive to changes in π-acidity, whereas anion−π interactions with a virtual carbanion intermediate increase dramatically with increasing π-acidity of the catalyst. Taken together, these findings rule out significant contributions from π−π interactions and provide compelling corroborative experimental evidence for the existence of anion−π catalysis.

Evidence that anion−π interactions can contribute to organocatalysis could influence the field in the broadest sense. Focused heavily on hydrogen bonds, the ongoing shift of attention toward other established interactions, such as ion pairing[17] or cation−π interactions,[16] as well as toward the more innovative halogen bonds[12,18] provides marvelous examples how the introduction of new interaction can inspire the field beyond incremental progress. Catalysis with anion−π interactions is entirely new. The Kemp elimination is obviously not interesting for organocatalysis and used in this study as the (ideal) tool rather than the (irrelevant) topic. However, stabilization of the anionic transition state of the Kemp elimination implies that anion−π interactions can stabilize anionic transition states in the broadest sense. Enolate chemistry is particularly interesting for anion−π catalysis. Claisen condensations with anionic transition states dominate polyketide biosynthesis[33] as carbocation chemistry dominates terpenoid and steroid biosynthesis,[13,14] and it would certainly be intriguing if anion−π interactions could complement the central role cation−π interactions play in stabilizing carbocation intermediates. Intense studies to expand anion−π catalysis beyond the Kemp elimination are ongoing, and the first results will be reported soon.

■ ASSOCIATED CONTENT

Supporting Information

Experimental details. This material is available free of charge via the Internet at http://pubs.acs.org.

■ AUTHOR INFORMATION

Corresponding Author

stefan.matile@unige.ch

Notes

The authors declare no competing financial interest.

■ ACKNOWLEDGMENTS

We thank D. Jeannerat, A. Pinto, and S. Grass for NMR measurements, the Sciences Mass Spectrometry (SMS) platform for mass spectrometry services, and the University of Geneva, the European Research Council (ERC Advanced Investigator), the National Centre of Competence in Research (NCCR) Chemical Biology, and the Swiss NSF for financial support.

■ REFERENCES

(1) (a) Quinonero, D.; Garau, C.; Rotger, C.; Frontera, A.; Ballester, P.; Costa, A.; Deya, P. M. *Angew. Chem., Int. Ed.* **2002**, *41*, 3389−3392. (b) Mascal, M.; Armstrong, A.; Bartberger, M. D. *J. Am. Chem. Soc.* **2002**, *124*, 6274−6276. (c) Alkorta, I.; Rozas, I.; Elguero, J. *J. Am. Chem. Soc.* **2002**, *124*, 8593−8598.

(2) (a) Frontera, A.; Gamez, P.; Mascal, M.; Mooibroek, T. J.; Reedijk, J. *Angew. Chem., Int. Ed.* **2011**, *50*, 9564−9583. (b) Chifotides, H. T.; Dunbar, K. R. *Acc. Chem. Res.* **2013**, *46*, 894−906. (c) Gamez, P.; Mooibroek, T. J.; Teat, S. J.; Reedijk, J. *Acc. Chem. Res.* **2007**, *40*, 435−444. (d) Salonen, L. M.; Ellermann, M.; Diederich, F. *Angew. Chem., Int. Ed.* **2011**, *50*, 4808−4842. (e) Schneider, H.-J. *Acc. Chem. Res.* **2013**, *46*, 1010−1019. (f) Giese, M.; Albrecht, M.; Krappitz, T.; Peter, M.; Gossen, V.; Raabe, G.; Valkonen, A.; Rissanen, K. *Chem. Commun.* **2012**, *48*, 9983−9985. (g) Wheeler, S. E.; Houk, K. N. *J. Phys. Chem. A* **2010**, *114*, 8658−8664. (h) Hay, B. P.; Custelcean, R. *Cryst. Growth. Des.* **2009**, *9*, 2539−2545. (i) Schneebeli, S. T.; Frasconi, M.; Liu, Z.; Wu, Y.; Gardner, D. M.; Strutt, N. L.; Cheng, C.; Carmieli, R.; Wasielewski, M. R.; Stoddart, J. F. *Angew. Chem., Int. Ed.* **2013**, *52*, 13100−13104.

(3) (a) Ballester, P. *Acc. Chem. Res.* **2013**, *46*, 874−884. (b) Wang, D.-X.; Wang, M.-X. *J. Am. Chem. Soc.* **2013**, *135*, 892−897. (c) Watt, M. M.; Zakharov, L. N.; Haley, M. M.; Johnson, D. W. *Angew. Chem., Int. Ed.* **2013**, *52*, 10275−10280. (d) Arranz-Mascroś, P.; Bazzicalupi, C.; Bianchi, A.; Giorgi, C.; Godino-Salido, M.-L.; Gutieŕrez-Valero, M.-D.; Lopez-Garzoń, R.; Savastano, M. *J. Am. Chem. Soc.* **2013**, *135*, 102−105. (e) Barceló-Oliver, M.; Bauzá, A.; Baquero, B. A.; García-Raso, A.; Terrón, A.; Molins, E.; Frontera, A. *Tetrahedron Lett.* **2013**, *54*, 5355−5360. (f) Cadman, C. J.; Croft, A. K. *Beilstein J. Org. Chem.* **2011**, *7*, 320−328. (g) Chudzinski, M. G.; McClary, C. A.; Taylor, M. S. *J. Am. Chem. Soc.* **2011**, *133*, 10559−10567. (h) Wang, D.-X.; Zheng, Q. Y.; Wang, Q. Q.; Wang, M.-X. *Angew. Chem., Int. Ed.* **2008**, *47*, 7485−7488. (i) Maeda, H.; Morimoto, T.; Osuka, A.; Furuta, H. *Chem. Asian J.* **2006**, *1*, 832−844. (j) Rosokha, Y. S.; Lindeman, S. V.; Rosokha, S. V.; Kochi, J. K. *Angew. Chem., Int. Ed.* **2004**, *43*, 4650−4652.

(4) (a) Bhosale, S. V.; Jani, C. H.; Langford, S. J. *Chem. Soc. Rev.* **2008**, *37*, 331−342. (b) Sakai, N.; Mareda, J.; Vauthey, E.; Matile, S. *Chem. Commun.* **2010**, *46*, 4225−4237. (c) Bhosale, S. V.; Bhosale, S. V.; Bhargava, S. K. *Org. Biomol. Chem.* **2012**, *10*, 6455−6468. (d) Takai, A.; Yasuda, T.; Ishizuka, T.; Kojima, T.; Takeuchi, M. *Angew. Chem., Int. Ed.* **2013**, *52*, 9167−9171. (e) Avinash, M. B.; Samanta, P. K.; Sandeepa, K. V.; Pati, S. K.; Govindaraju, T. *Eur. J. Org. Chem.* **2013**, 5838−5847. (f) Doria, F.; Manet, I.; Grande, V.; Monti, S.; Freccero, M. *J. Org. Chem.* **2013**, *78*, 8065−8073. (g) Fukutomi, Y.; Nakano, M.; Hu, J.-Y.; Osaka, I.; Takimiya, K. *J. Am. Chem. Soc.* **2013**, *135*, 11445−11448. (h) Zhang, F.; Hu, Y.; Schuettfort, T.; Di, C.-A.; Gao, X.; McNeill, C. R.; Thomsen, L.; Mannsfeld, S. C. B.; Yuan, W.; Sirringhaus, H.; Zhu, D. *J. Am. Chem. Soc.* **2013**, *135*, 2338−2349. (i) Ponnuswamy, N.; Pantoş, G. D.; Smulders, M. M. J.; Sanders, J. M. K. *J. Am. Chem. Soc.* **2012**, *134*, 566−573. (j) Molla, M. R.; Ghosh, S. *Chem.—Eur. J.* **2012**, *18*, 9860−9869. (k) Chong, Y. S.; Dial, B. E.; Burns, W. G.; Shimizu, K. D. *Chem. Commun.* **2012**, *48*, 1296−1298. (l) Cai, K.; Yan, Q.; Zhao, D. *Chem. Sci.* **2012**, *3*, 3175−3182. (m) Collie, G. W.; Promontorio, R.; Hampel, S. M.; Micco, M.; Neidle, S.; Parkinson, G. N. *J. Am. Chem. Soc.* **2012**, *134*, 2723−2731. (n) Würthner, F.; Stolte, M. *Chem. Commun.* **2011**, *47*, 5109−5115. (o) Holman, G. G.; Zewail-Foote, M.; Smith, A. R.; Johnson, K. A.; Iverson, B. L. *Nat. Chem.* **2011**, *3*, 875−881. (p) Tu, S.; Kim, S. H.; Joseph, J.; Modarelli, D. A.; Parquette, J. L. *J. Am. Chem. Soc.* **2011**, *133*, 19125−19130. (q) Liu, K.; Wang, C.; Li, Z.; Zhang, X. *Angew. Chem., Int. Ed.* **2011**, *50*, 4952−4956. (r) Yue, W.; Gao, J.; Li, Y.; Jiang, W.; Di Motta, S.; Negri, F.; Wang, Z. *J. Am. Chem. Soc.* **2011**, *133*, 18054−18057. (s) Zhan, X.; Facchetti, A.; Barlow, S.; Marks, T. J.; Ratner, M. A.; Wasielewski, M. R.; Marder, S. R. *Adv. Mater.* **2011**, *23*, 268−284. (t) Sakai, N.; Lista, M.; Kel, O.; Sakurai, S.; Emery, D.;

Mareda, J.; Vauthey, E.; Matile, S. *J. Am. Chem. Soc.* **2011**, *133*, 15224−15227. (u) Murase, T.; Otsuka, K.; Fujita, M. *J. Am. Chem. Soc.* **2010**, *132*, 7864−7865. (v) Burattini, S.; Greenland, B. W.; Merino, D. H.; Weng, W.; Seppala, J.; Colquhoun, H. M.; Hayes, W.; Mackay, M. E.; Hamley, I. W.; Rowan, S. J. *J. Am. Chem. Soc.* **2010**, *132*, 12051−12058. (w) Krüger, H.; Janietz, S.; Sainova, D.; Dobreva, D.; Koch, N.; Vollmer, A. *Adv. Funct. Mater.* **2007**, *17*, 3715−3723. (x) Jones, B. A.; Facchetti, A.; Wasielewski, M. R.; Marks, T. J. *J. Am. Chem. Soc.* **2007**, *129*, 15259−15278. (y) Sakai, N.; Sisson, A. L.; Bürgi, T.; Matile, S. *J. Am. Chem. Soc.* **2007**, *129*, 15758−15759. (z) Tanaka, H.; Litvinchuk, S.; Tran, D.-H.; Bollot, G.; Mareda, J.; Sakai, N.; Matile, S. *J. Am. Chem. Soc.* **2006**, *128*, 16000−16001. (aa) Talukdar, P.; Bollot, G.; Mareda, J.; Sakai, N.; Matile, S. *Chem.—Eur. J.* **2005**, *11*, 6525−6532. (bb) Abraham, B.; McMasters, S.; Mullan, M. A.; Kelly, L. A. *J. Am. Chem. Soc.* **2004**, *126*, 4293−4300. (cc) Würthner, F.; Ahmed, S.; Thalacker, C.; Debaerdemaeker, T. *Chem.—Eur. J.* **2002**, *8*, 4742−4750. (dd) Katz, H. E.; Lovinger, A. J.; Johnson, J.; Kloc, C.; Siegrist, T.; Li, W.; Lin, Y. Y.; Dodabalapur, A. *Nature* **2000**, *404*, 478−481. (ee) Miller, L. L.; Mann, K. R. *Acc. Chem. Res.* **1996**, *29*, 417−423.

(5) Gorteau, V.; Bollot, G.; Mareda, J.; Perez-Velasco, A.; Matile, S. *J. Am. Chem. Soc.* **2006**, *128*, 14788−14789.

(6) Dawson, R. E.; Hennig, A.; Weimann, D. P.; Emery, D.; Ravikumar, V.; Montenegro, J.; Takeuchi, T.; Gabutti, S.; Mayor, M.; Mareda, J.; Schalley, C. A.; Matile, S. *Nat. Chem.* **2010**, *2*, 533−538.

(7) Chang, J.; Ye, Q.; Huang, K.-W.; Zhang, J.; Chen, Z.-K.; Wu, J.; Chi, C. *Org. Lett.* **2012**, *14*, 2964−2967.

(8) Misek, J.; Vargas Jentzsch, A.; Sakurai, S.; Emery, D.; Mareda, J.; Matile, S. *Angew. Chem., Int. Ed.* **2010**, *49*, 7680−7683.

(9) Lin, N.-T.; Vargas Jentzsch, A.; Guénée, L.; Neudörfl, J.-M.; Aziz, S.; Berkessel, A.; Orentas, E.; Sakai, N.; Matile, S. *Chem. Sci.* **2012**, *3*, 1121−1127.

(10) Kishore, R. S. K.; Kel, O.; Banerji, N.; Emery, D.; Bollot, G.; Mareda, J.; Gomez-Casado, A.; Jonkheijm, P.; Huskens, J.; Maroni, P.; Borkovec, M.; Vauthey, E.; Sakai, N.; Matile, S. *J. Am. Chem. Soc.* **2009**, *131*, 11106−11116.

(11) (a) Würthner, F. *Chem. Commun.* **2004**, *40*, 1564−1579. (b) Shaller, A. D.; Wang, W.; Gan, H.; Li, A. D. Q. *Angew. Chem., Int. Ed.* **2008**, *47*, 7705−7709. (c) Jonkheijm, P.; Stutzmann, N.; Chen, Z.; de Leeuw, D. M.; Meijer, E. W.; Schenning, A. P. H. J.; Würthner, F. *J. Am. Chem. Soc.* **2006**, *128*, 9535−9540. (d) Sugiyasu, K.; Kawano, S.; Fujita, N.; Shinkai, S. *Chem. Mater.* **2008**, *20*, 2863−2865. (e) Charbonnaz, P.; Sakai, N.; Matile, S. *Chem. Sci.* **2012**, *3*, 1492−1496. (f) Giaimo, J. M.; Gusev, A. V.; Wasielewski, M. R. *J. Am. Chem. Soc.* **2002**, *124*, 8530−8531. (g) Perez-Velasco, A.; Gorteau, V.; Matile, S. *Angew. Chem., Int. Ed.* **2008**, *47*, 921−923.

(12) (a) Vargas Jentzsch, A.; Emery, D.; Mareda, J.; Metrangolo, P.; Resnati, G.; Matile, S. *Angew. Chem., Int. Ed.* **2011**, *50*, 11675−11678. (b) Vargas Jentzsch, A.; Emery, D.; Mareda, J.; Nayak, S. K.; Metrangolo, P.; Resnati, G.; Sakai, N.; Matile, S. *Nat. Commun.* **2012**, *3*, 905. (c) Vargas Jentzsch, A.; Matile, S. *J. Am. Chem. Soc.* **2013**, *135*, 5302−5303. (d) Adriaenssens, L.; Estarellas, C.; Vargas Jentzsch, A.; Martinez Belmonte, M.; Matile, S.; Ballester, P. *J. Am. Chem. Soc.* **2013**, *135*, 8324−8330. (e) Vargas Jentzsch, A.; Hennig, A.; Mareda, J.; Matile, S. *Acc. Chem. Res.* **2013**, *46*, 2791−2800.

(13) (a) Dougherty, D. A. *Acc. Chem. Res.* **2013**, *46*, 885−893. (b) Mahadevi, A. S.; Sastry, G. N. *Chem. Rev.* **2013**, *113*, 2100−2138.

(14) Wendt, K. U.; Schulz, G. E.; Corey, E. J.; Liu, D. R. *Angew. Chem., Int. Ed.* **2000**, *39*, 2812−2833.

(15) (a) Yamada, S.; Fossey, J. S. *Org. Biomol. Chem.* **2011**, *9*, 7275−7281. (b) Stauffer, D. A.; Barrans, R. E., Jr.; Dougherty, D. A. *Angew. Chem., Int. Ed.* **1990**, *29*, 915−918. (c) McCurdy, A.; Jimenez, L.; Stauffer, D. A.; Dougherty, D. A. *J. Am. Chem. Soc.* **1992**, *114*, 10314−10321. (d) P. Lakshminarasimhan, P.; Sunoj, R. B.; Chandrasekhar, J.; Ramamurthy, V. *J. Am. Chem. Soc.* **2000**, *122*, 4815−4816. (e) Neda, I.; Sakhaii, P.; Wassmann, A.; Niemeyer, U.; Günther, E.; Engel, J. *Synthesis* **1999**, 1625−1632. (f) Yao, L.; Aubé, J. *J. Am. Chem. Soc.* **2007**, *129*, 2766−2767. (g) Knowles, R. R.; Lin, S.; Jacobsen, E. N. *J. Am. Chem. Soc.* **2010**, *132*, 5030−5032. (h) Lin, S.; Jacobsen, E. N. *Nat. Chem.* **2012**, *4*, 817−824.

(16) (a) Rojas, C. M.; Rebek, J., Jr. *J. Am. Chem. Soc.* **1998**, *120*, 5120−5121. (b) Estarellas, C.; Frontera, A.; Quiñonero, D.; Deyà, P. M. *Angew. Chem., Int. Ed.* **2011**, *50*, 415−418. (c) Phuengphai, P.; Youngme, S.; Mutikainen, I.; Reedijk, J. *Inorg. Chem. Commun.* **2012**, *24*, 129−133.

(17) (a) Mahlau, M.; List, B. *Angew. Chem., Int. Ed.* **2013**, *52*, 518−533. (b) Brak, K.; Jacobsen, E. N. *Angew. Chem., Int. Ed.* **2013**, *52*, 534−561. (c) Phipps, R. J.; Hamilton, G. L.; Toste, F. D. *Nat. Chem.* **2012**, *4*, 603−614. (d) Lacour, J.; Moraleda, D. *Chem. Commun.* **2009**, 7073−7089. (e) Sakai, N.; Matile, S. *J. Am. Chem. Soc.* **2003**, *125*, 14348−14356.

(18) (a) Bruckmann, A.; Pena, M. A.; Bolm, C. *Synlett* **2008**, *6*, 900−902. (b) Kraut, D. A.; Churchil, M. J.; Dawson, P. E.; Herschlag, D. *ACS Chem. Biol.* **2009**, *4*, 269−273. (c) Coulembier, O.; Meyer, F.; Dubois, P. *Polym. Chem.* **2010**, *1*, 434−437. (d) Walter, S.; Kniep, F.; Herdtweck, E.; Huber, S. M. *Angew. Chem., Int. Ed.* **2011**, *50*, 7187−7191. (e) Lindsay, V. N. G.; Charette, A. B. *ACS Cat.* **2012**, *2*, 1221−1225. (f) Kniep, F.; Jungbauer, S. H.; Zhang, Q.; Walter, S. M.; Schindler, S.; Schnapperelle, I.; Herdtweck, E.; Huber, S. M. *Angew. Chem., Int. Ed.* **2013**, *52*, 7028−7032.

(19) (a) Li, J.; Nowak, P.; Otto, S. *J. Am. Chem. Soc.* **2013**, *135*, 9222−9239. (b) Cougnon, F. B. L.; Sanders, J. K. M. *Acc. Chem. Res.* **2012**, *45*, 2211−2221. (c) Lehn, J.-M. *Top. Curr. Chem.* **2012**, *322*, 1−32. (d) Gasparini, G.; Prins, L. J.; Scrimin, P. *Angew. Chem., Int. Ed.* **2008**, *47*, 2475−2479. (e) Wilson, A.; Gasparini, G.; Matile, S. *Chem. Soc. Rev.*, DOI: 10.1039/C3CS60342C.

(20) Zhao, Y.; Domoto, Y.; Orentas, E.; Beuchat, C.; Emery, D.; Mareda, J.; Sakai, N.; Matile, S. *Angew. Chem., Int. Ed.* **2013**, *52*, 9940−9943.

(21) (a) Röthlisberger, D.; Khersonsky, O.; Wollacott, A. M.; Jiang, L.; DeChancie, J.; Betker, J.; Gallaher, J. L.; Althoff, E. A.; Zanghellini, A.; Dym, O.; Albeck, S.; Houk, K. N.; Tawfik, D. S.; Baker, D. *Nature* **2008**, *453*, 190−195. (b) Hu, Y.; Houk, K. N.; Kikuchi, K.; Hotta, K.; Hilvert, D. *J. Am. Chem. Soc.* **2004**, *126*, 8197−8205. (c) Kennan, A. J.; Whitlock, H. W. *J. Am. Chem. Soc.* **1996**, *118*, 3027−3028. (d) Hollfelder, F.; Kirby, A. J.; Tawfik, D. S. *J. Org. Chem.* **2001**, *66*, 5866−5874. (e) Merski, M.; Shoichet, B. K. *Proc. Natl. Acad. Sci. U.S.A.* **2012**, *109*, 16179−16183. (f) Klijn, J. E.; Engberts, J. B. F. N. *Org. Biomol. Chem.* **2004**, *2*, 1789−1799. (g) Alexandrova, A. N.; Jorgensen, W. L. *J. Phys. Chem. B* **2009**, *113*, 497−504. (h) Frushicheva, M. P.; Cao, J.; Warshel, A. *Biochemistry* **2011**, *50*, 3849−3858.

(22) Wolfenden, R.; Snider, M. J. *Acc. Chem. Res.* **2001**, *34*, 938−945.

(23) Grimme, S. *J. Comput. Chem.* **2006**, *27*, 1787−1799.

(24) Zhao, Y.; Truhlar, D. G. *Theor. Chem. Acc.* **2008**, *120*, 215−241.

(25) (a) Tomasi, J.; Mennucci, B.; Cammi, R. *Chem. Rev.* **2005**, *105*, 2999−3093. (b) Cances, E.; Mennucci, B.; Tomasi, J. *J. Chem. Phys.* **1997**, *107*, 3032−3041.

(26) Estarellas, C.; Bauza, A.; Frontera, A.; Quinonero, D.; Deya, P. M. *Phys. Chem. Chem. Phys.* **2011**, *13*, 16698−16705.

(27) (a) Sakai, N.; Matile, S. *J. Am. Chem. Soc.* **2002**, *124*, 1184−1185. (b) Sakai, N.; Gerard, D.; Matile, S. *J. Am. Chem. Soc.* **2001**, *123*, 2517−2524.

(28) Suseela, Y. V.; Sasikumar, M.; Govindaraju, T. *Tetrahedron Lett.* **2013**, *54*, 6314−6318.

(29) (a) Browne, D. T.; Eisinger, J.; Leonard, N. J. *J. Am. Chem. Soc.* **1968**, *90*, 7302−7323. (b) Leonard, N. J. *Acc. Chem. Res.* **1979**, *12*, 423−429. (c) Garcia-Raso, A.; Fiol, J. J.; Badenas, F.; Solans, X.; Font-Bardia, M. *Polyhedron* **1999**, *18*, 765−772.

(30) (a) Avasthi, K.; Chandra, T.; Bhakuni, D. S. *Indian J. Chem.* **1995**, *34B*, 944−949. (b) Avasthi, K.; Ansari, A.; Tewari, A. K.; Kant, R.; Maulik, P. R. *Org. Lett.* **2009**, *11*, 5290−5293.

(31) Richter, I.; Minari, J.; Axe, P.; Lowe, J. P.; James, T. D.; Sakurai, K.; Bull, S. D.; Fossey, J. S. *Chem. Commun.* **2008**, *44*, 1082−1084.

(32) Takeuchi, T.; Kosuge, M.; Tadokoro, A.; Sugiura, Y.; Nishi, M.; Kawata, M.; Sakai, N.; Matile, S.; Futaki, S. *ACS Chem. Biol.* **2006**, *1*, 299−303.

(33) (a) Walker, M. C.; Thuronyi, B. W.; Charkoudian, L. K.; Lowry, B.; Khosla, C.; Chang, M. C *Science* **2013**, *341*, 1089−1094. (b) Bretschneider, T.; Heim, J. B.; Heine, D.; Winkler, R.; Busch,

B.; Kusebauch, B.; Stehle, T.; Zocher, G.; Hertweck, C. *Nature* **2013**, *502*, 124−128. (c) Cane, D. E.; Walsh, C. T.; Khosla, C. *Science* **1998**, *282*, 63−68. (d) Jenni, S.; Leibundgut, M.; Boehringer, D.; Frick, C.; Mikolásek, B.; Ban, N. *Science* **2007**, *316*, 254−261.